VIROLOGY 95, 359–372 (1979)

Restriction Endonuclease *Hin*dIII Cleavage Site Map of Bacteriophage P22

ROBERT J. DEANS AND ETHEL NOLAND JACKSON[1]

Department of Microbiology, University of Michigan, Ann Arbor, Michigan 48109

Accepted January 22, 1979

The 14 *Hin*dIII cleavage sites on P22 DNA have been mapped. *Hin*dIII cleavage sites were located relative to *Eco*RI sites by determining the molecular weights and map order of fragments produced by *Hin*dIII, or *Hin*dIII and *Eco*RI digestion. Molecular weights were estimated from the electrophoretic mobility of fragments. The *Hin*dIII fragment order was established by *Hin*dIII cleavage of segments of the P22 genome obtained as isolated *Eco*RI fragments or as overlapping genetic substitutions in bacteriophage λ chromosomes. The resulting *Hin*dIII/*Eco*RI cleavage site map defines physical markers in all regions of the P22 genome and defines the locations of a number of P22 genes on this physical map of the P22 chromosome. Three *Hin*dIII sites and two *Hpa*I sites have been mapped in *imm*I, one of two P22 gene clusters controlling lysogeny. Two of these *Hin*dIII sites lie within the structural gene *ant* specifying one of the regulatory proteins of the *imm*I region. Assignment of the *ant* gene to specific *Hin*dIII fragments utilized the insertion element Tnl, which was shown to contain no *Hin*dIII cleavage sites.

INTRODUCTION

Restriction endonucleases which cleave double-stranded DNA at a specific nucleotide sequence are valuable tools in the study of genome structure and organization, since they provide physical markers on the chromosome (Nathans and Smith, 1975). Analysis of the DNA of bacteriophage P22 by cleavage with the restriction endonuclease *Eco*RI has recently provided new insights into the way in which the concatemer produced by P22 DNA replication is processed to yield the mature linear form of the viral chromosome found in virus particles (Jackson *et al.*, 1978a, b). The map of the seven *Eco*RI cleavage sites in P22 DNA which was generated in those studies was also the beginning of a physical gene map which will aid further study of the organization and function of P22 genes. However, *Eco*RI cleavage sites are distributed unevenly on the P22 chromosome. Almost 50% of the genome is contained in one *Eco*RI fragment, and another 20% in a second fragment. We wished to locate additional restriction enzyme cleavage sites to provide more physical markers on the chromosome. Therefore, in order to further dissect the P22 genome, we chose restriction endonuclease *Hin*dIII.

*Hin*dIII cleavage sites were mapped relative to *Eco*RI cleavage sites on the P22 chromosome by analyzing products of *Hin*dIII digestion of individual P22 *Eco*RI restriction fragments. When more than two *Hin*dIII sites were contained in a single *Eco*RI fragment, the *Hin*dIII cleavage sites were oriented by cleavage with a third enzyme, or by cleavage of hybrid DNA molecules in which only a portion of the P22 fragment under study was substituted into a bacteriophage λ chromosome. By these methods, restriction endonuclease cleavage sites have been mapped in all regions of the P22 chromosome, and a number of P22 genes have been placed relative to these physical markers.

MATERIALS AND METHODS

Bacteriophage and bacterial stains. Bacteriophage P22 *c*1-7 was obtained from M. Levine and was the source of wild-type

[1] To whom requests for reprints should be addressed.

0042-6822/79/080359-14$02.00/0
Copyright © 1979 by Academic Press, Inc.
All rights of reproduction in any form reserved.

P22 DNA. P22 bp5 *c2am5* 13⁻*am*H101, obtained from D. Botstein, carries a deletion of a region of the P22 genome not essential for lytic growth, as well as amber mutations in genes for phage repressor (*c2*) and lysis function (gene 13) (Chan and Botstein, 1976).

λ*imm*P22 hybrids were obtained from D. Botstein and S. Hilliker. λ*imm*P22hyl, described by Botstein and Herskowitz (1974), carries P22 genes 24, *c2*, 18, and 12 in place of λ genes N, cI, O, and P. The P22 substitution in λ*imm*P22hy38 *c2-5* 13⁻*am*H101 has been shown to include at least P22 genes 24, *c2*, 18, 12, and 13 (S. Hilliker, personal communication). The P22 substitution in λ*imm*P22hy37 includes at least P22 genes 24, *c2*, 18, and 12, and exhibits a *spi*⁻ phenotype (S. Hilliker, 1974; Zissler *et al.*, 1971).

Derivatives of *Salmonella typhimurium* LT2 *su*⁻ *leu*A⁻ which were lysogenic for P22 carrying the Tnl insertion element (Heffron *et al.*, 1975; Hernalsteens *et al.*, 1977) in various P22 genes were obtained from G. Weinstock and D. Botstein (Weinstock, 1977). P22 phage obtained following uv induction of these lysogens are designated P22 Ap (to indicate the presence of the ampicillin resistant Tnl insertion). The P22 Ap strains used here carry Tnl in P22 genes *ant* (P22 Ap29, Ap63, Ap4, Ap24, Ap9) or gene 9 (P22 Ap25, Ap7) (Weinstock, 1977).

S. typhimurium LT2 strain 18, a standard *su*⁻ prototroph, and strain 325, which carries an amber suppressor, were both obtained from M. Levine.

Escherichia coli K12 strain W3110, a standard *su*⁻ prototroph, and *E. coli* K12 strain Ymel *su*III, which carries an amber suppressor, are from the collection of C. Yanofsky. The lysogen *E. coli* W3102 *gal*⁻ *str*ʳ (λcI857 *Sam7*) was obtained from D. Friedman.

E. coli K12 *met*⁻ *rk*⁻ *mk*⁺ *su*II *su*III *trp*R⁻/pP22-6 (Chisholm, Deans, Jackson, and Jackson, manuscript in preparation) carries a plasmid produced by *in vitro* ligation of P22 *Eco*RI fragment E at the single *Eco*RI site in plasmid pBR322 (Bolivar *et al.*, 1977). *E. coli* K12 *met*⁻ *rk*⁻ *mk*⁺ *su*II *su*III *trp*R⁻/pP22-7 carries a plasmid similarly constructed which contains P22 *Eco*RI G (Chisholm, Deans, Jackson, and Jackson, manuscript in preparation).

Bacteriophage lysates and DNA preparations. Lysates of λ and P22 were prepared by lytic infection, temperature induction, or uv induction as described by Jackson *et al.* (1978a, b). DNA was prepared from these lysates as described by Jackson *et al.* (1978a, b). Growth of *S. typhimurium* lysogenic for P22 prophages containing the ampicillin resistance element Tnl was performed in L broth supplemented with 50 μg/ml ampicillin (Sigma). Plasmid DNA was prepared and purified as described by Collins *et al.* (1976). SV40 DNA was a gift of Robert Deleys.

Restriction endonucleolytic cleavage reactions. *Eco*RI was purified according to the method of Thomas and Davis (1975). Reactions were carried out in 6 m*M* Tris–HCl (pH 7.5), 6 m*M* $MgCl_2$, 50 m*M* NaCl, and 50 μg/ml gelatin at 37° for 1 hr. With 1 μl of enzyme, 0.5 to 1.5 μg of P22 DNA was digested to completion in 20- to 50-μl reaction volumes. Larger amounts of P22 DNA up to 500 μg were digested in 1.5- to 2.0-ml volumes under these reaction conditions.

*Hin*dIII was a gift from W. Folk. Reaction conditions for *Hin*dIII and *Eco*RI/*Hin*dIII double digestions were identical for those described for *Eco*RI.

*Hpa*I was a gift of D. Mason. P22 DNA (1.6 μg) was digested in a reaction volume of 25 μl consisting of 10 m*M* Tris–HCl (pH 7.5), 10 m*M* $MgCl_2$, 6 m*M* β-mercaptoethanol, 6 m*M* KCl, and 60 μg/ml gelatin. Reactions were performed for 1 hr at 37°. Cleavage by *Hin*dIII plus *Hpa*I was achieved by first incubating DNA and *Hin*dIII for 30 min at 37° in 6 m*M* Tris–HCl (pH 7.5), 6 m*M* $MgCl_2$, 50 m*M* NaCl, 50 μg/ml gelatin followed by addition of *Hpa*I, and KCl to 10 m*M*, for an additional 30 min at 37°.

All restriction endonuclease reactions were terminated by the addition of 0.10 vol of 25% Ficoll 400 (Pharmacia), 0.0025% bromophenol blue (Eastman), and 100 m*M* EDTA.

Agarose gel electrophoresis. Samples of 20 to 50 μl containing 0.5 to 1.5 μg of DNA were analyzed by electrophoresis in 24 × 13 × 0.45-cm agarose (0.7%) slab gels as de-

scribed previously (Deleys and Jackson, 1976; Jackson *et al.*, 1978b). Electrophoresis was performed at 30 V for 15 hr at room temperature, and the gel was stained with ethidium bromide and photographed as described previously (Jackson *et al.*, 1978b). Preparative scale gel electrophoresis of 250 μg DNA was accomplished by the same procedure except that the DNA sample, in a total volume not exceeding 2 ml, was layered on the gel in a single well.

Polyacrylamide gel electrophoresis. Electrophoresis was performed in a 4% polyacrylamide gel as described by Lai and Nathans (1974). The dimensions and buffer systems of the agarose gel electrophoresis system were employed. All reagents were purchased from Eastman Chemical Company. Samples were made 0.1% SDS prior to loading on the gel. Electrophoresis was performed at 50 V for 15 hr. The gels were removed and stained in 10 μg/ml ethidium bromide for 20 min, then destained in water for 20 min at 4°. Visualization of DNA bands and photography were performed as described previously for agarose gel electrophoresis (Jackson *et al.*, 1978b).

DNA fragment purification. *Eco*RI cleavage products of 250 μg P22 DNA were separated by electrophoresis in an agarose slab gel and stained as described above. The DNA bands were located by fluorescence of the bound ethidium bromide in long wavelength ultraviolet light, and the region of the gel containing a band was cut out and passed through 18-, 20-, and 25-gauge syringe needles successively. This mixture was transferred to a ⅝ × 3-in. cellulose nitrate tube, filled with electrophoresis buffer, and allowed to stand at room temperature at least 6 hr. The sample was centrifuged in a Beckman 50 Ti rotor at 20,000 rpm for 40 min at 4°. The supernatant was then precipitated by the addition of 2 vol of ethanol, and the precipitate was collected by centrifugation at 22,000 rpm for 30 min at 4° in a Beckman SW 27 rotor. The DNA was then purified in an isopycnic CsCl-ethidium bromide gradient, as described by Collins *et al.* (1976). The tubes were illuminated with a hand-held ultraviolet light source, and the fluorescent DNA/ethidium bromide band was collected through the side of the tube with a sterile syringe and 25-gauge needle, extracted twice with NaCl-saturated isopropanol, and dialyzed into 10 m*M* Tris–HCl (pH 8.1), 10 m*M* NaCl, 1 m*M* EDTA. *Eco*RI DNA fragments purified by this procedure could be cleaved with the restriction enzymes *Hin*dIII and *Hpa*I. The final yield of DNA was usually between 60 and 80%.

Nomenclature. Bands appearing following gel electrophoresis of *Eco*RI or *Hin*dIII digests of P22 DNA are assigned letter designations according to conventions outlined previously (Smith and Nathans, 1973; Jackson *et al.*, 1978a). Bands which are produced by digestion with both *Eco*RI and *Hin*dIII and which are not found following cleavage with either enzyme alone are assigned lower case letters in order of increasing electrophoretic mobility.

RESULTS

HindIII Cleavage Products of P22 DNA

Circularly permuted, linear P22 DNA was extracted from viral particles, digested with *Hin*dIII, and the fragments separated by electrophoresis through agarose or polyacrylamide gels (Figs. 1c and f). The molecular weights of the fragments were estimated from comparisons of their electrophoretic mobilities with those of standard DNA molecules of known molecular weight. The 14 bands found following electrophoresis range in molecular weight from 0.2 to 10.3 × 10^6 daltons (Table 1).

*Eco*RI cleavage sites have been located on the P22 chromosome and this physical map has been oriented relative to the P22 genetic map (Jackson *et al.*, 1978a, b). Therefore, *Hin*dIII cleavage sites were mapped relative to *Eco*RI sites on P22 DNA. The products of cleavage of P22 DNA with both *Eco*RI and *Hin*dIII were compared with the products of digestion with either enzyme alone (Fig. 1). *Eco*RI fragments B, D, and H appear intact in the double digest, and so contain no *Hin*dIII cleavage sites. All other *Eco*RI fragments contain at least one *Hin*dIII site. Similarly, *Hin*dIII fragments D, E, F, G, J, K, L, M, and N appear to contain no *Eco*RI restriction targets.

*Hin*dIII sites were mapped between two

particular P22 *Eco*RI sites by purifying a given *Eco*RI fragment free of other P22 *Eco*RI fragments, and then cleaving it with *Hin*dIII and comparing the resulting cleavage products with the products of *Hin*dIII or *Eco*RI/*Hin*dIII double digestion of whole P22 DNA. This approach was used to map *Hin*dIII sites in *Eco*RI fragments A, C, E, and G. As expected, purified *Eco*RI fragments B, D, and H were not cleaved when incubated with *Hin*dIII.

HindIII cleavage products of P22 EcoRI A. Seven fragments appear after digestion of P22 *Eco*RI A with *Hin*dIII. Five of the fragments comigrate with P22 *Hin*dIII fragments D, E, F, G, and J (data not shown). The remaining two fragments (*Eco*RI/*Hin*dIII fragments b and c) appear only when P22 DNA is cleaved with both *Eco*RI and *Hin*dIII, and therefore arise from the ends of P22 *Eco*RI A.

P22 *Eco*RI D (defined at physical map coordinates 0–.096 as shown in Fig. 5) is derived from one end of P22 *Eco*RI A during packaging of DNA into the P22 head (Jackson *et al.*, 1978a, b). Since P22 *Eco*RI D is not cleaved by *Hin*dIII, there are no *Hin*dIII cleavage sites between map coordinates 0 and .096 (2.65×10^6 daltons). The size of the end fragment *Eco*RI/*Hin*dIII c is 2.0×10^6 daltons, and thus it cannot arise from the *Eco*RI D terminus of *Eco*RI A. *Eco*RI/*Hin*dIII c must therefore arise from the opposite end of *Eco*RI A. The

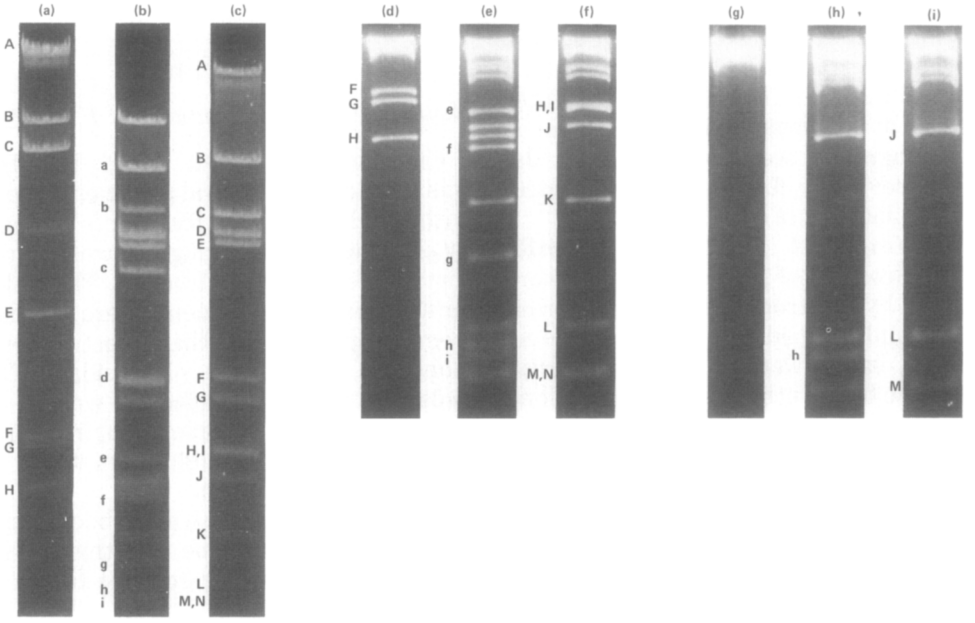

FIG. 1. Gel electrophoresis of *Eco*RI and *Hin*dIII cleavage products of P22 and P22 bp5 DNAs. (a–c) Agarose gel electrophoresis of P22 DNA cleaved by (a) *Eco*RI, (b) *Eco*RI plus *Hin*dIII, and (c) *Hin*dIII. (d–f) Polyacrylamide gel electrophoresis of P22 DNA cleaved by (d) *Eco*RI, (e) *Eco*RI plus *Hin*dIII, and (f) *Hin*dIII. (g–i) Polyacrylamide gel electrophoresis of P22 bp5 DNA (16% deletion) cleaved by (g) *Eco*RI, (h) *Eco*RI plus *Hin*dIII, and (i) *Hin*dIII. P22 or P22 bp5 DNA was digested with restriction endonucleases and the cleavage products were separated by electrophoresis as described under Materials and Methods. Fragments produced by digestion with a single restriction endonuclease are designated by capital letters in order of increasing electrophoretic mobility. Fragments generated by digestion with both *Eco*RI and *Hin*dIII are assigned lower case letters in order of increasing electrophoretic mobility and only these fragments are labeled in tracks (b), (e), and (h). P22 bp5 carries a deletion which covers P22 *Eco*RI sites 4, 5, and 6 (Fig. 5) and therefore results in the loss of P22 *Eco*RI fragments C, F, G, and H (Jackson *et al.*, 1978a). Similarly, P22 *Hin*dIII fragments H, I, K, N, and P22 *Eco*RI/*Hin*dIII double-digest fragments e, f, g, i, and j which are derived from the region deleted in P22 bp5 are also missing.

TABLE 1

MOLECULAR WEIGHTS OF *Hin*dIII AND *Eco*RI/*Hin*dIII CLEAVAGE PRODUCTS OF P22 DNA[a]

	Molecular weight ($\times 10^{-6}$ daltons)
P22 *Hin*dIII fragment	
A[b]	10.3
B	4.2
C	2.8
D	2.6
E	2.4
F	1.2
G	1.0
H	.65
I	.62
J	.50
K	.33
L	.23
M	.20
N	.20
P22 *Eco*RI/*Hin*dIII fragment	
a	4.07
b	3.1
c	2.0
d	1.1
e	.60
f	.55
g	.30
h	.22
i	.21
j[c]	—

[a] Molecular weights of P22 *Hin*dIII fragments were obtained by measuring the electrophoretic mobilities of the fragments and of standard DNA molecules in the same gel, and then applying the curve obtained relating mobility to the logarithm of the molecular weight of standard DNA molecules. Molecular weights of P22 *Hin*dIII fragments B through G were determined by comparison with the λ *Eco*RI and λ *Hin*dIII fragment (Thomas and Davis, 1975; Robinson and Landy, 1977). Molecular weights of P22 *Hin*dIII fragments H through L were determined relative to λ *Hin*dIII and SV40 *Hin*dIII (Lai and Nathans, 1974) standard fragments. Molecular weights of the P22 *Eco*RI/*Hin*dIII double digest fragments a through i were estimated by the same method, except that P22 *Eco*RI fragments B, D, and H (Jackson *et al.*, 1978a,b), and P22 *Hin*dIII fragments D, E, F, G, J, K, L, and M present in the same digest were used as standards. The sum of the molecular weight estimates for P22 *Hin*dIII fragments, 27.23 $\times 10^6$ daltons, is close to the total molecular weight of P22 *Eco*RI fragments, 27.45 $\times 10^6$ daltons (Jackson *et al.*, 1978a,b).

[b] The molecular weight of *Hin*dIII A is calculated from the sum of the molecular weights of P22 *Eco*RI B, and P22 *Eco*RI/*Hin*dIII fragments b and d which comprise *Hin*dIII A. This largest P22 *Hin*dIII fragment is not found intact when mature wild-type P22 DNA is cleaved with *Hin*dIII since it is shortened as a consequence of sequential headful packaging of concatemeric P22 DNA (see Discussion).

[c] Presence of a double-digest fragment of molecular weight less than 0.05×10^6 daltons has been inferred from the analysis of the *Hin*dIII digestion products of isolated P22 *Eco*RI G (see text). This fragment has not been detected in the gel electrophoresis conditions employed here.

molecular weight of *Eco*RI/*Hin*dIII c and the position of *Eco*RI site 7 locates *Hin*dIII cleavage site 9 at map coordinate .699 (Fig. 5). *Eco*RI/*Hin*dIII fragment b therefore overlaps P22 *Eco*RI D, and identifies the position of *Hin*dIII cleavage site 14 at .982 map units (Fig. 5).

*Hin*dIII sites 9 through 14 lie internal to P22 *Eco*RI A, and generate P22 *Hin*dIII fragments D, E, F, G, and J. These sites are more precisely located with *Eco*RI A by methods described in a later section.

HindIII cleavage products of P22 EcoRI C. Two fragments (*Eco*RI/*Hin*dIII a and e in Fig. 1) are produced by cleavage of purified *Eco*RI C with *Hin*dIII, indicating the presence of a single *Hin*dIII site within *Eco*RI C (data not shown). The molecular weights of these double digestion fragments (Table 1) place the *Hin*dIII site 0.6×10^6 daltons from one end or the other of *Eco*RI C, at map coordinates .530 or .398. This *Hin*dIII site was located at coordinate .530 by examination of P22 bp5. In this mutant of P22, a deletion extends from about .46 to about .62 on the P22 physical map (Fig. 5) and removes *Eco*RI sites 4, 5, and 6 (Chan and Botstein, 1976; Jackson *et al.*, 1978a, b). Since *Eco*RI/*Hin*dIII fragment e is not found among the products of an *Eco*RI/*Hin*dIII digestion of P22 bp5 DNA (Fig. 1h), the *Hin*dIII cleavage site in *Eco*RI fragment C must be located at .530 on the map of P22 wild-type DNA (Fig. 5).

HindIII cleavage products of P22 EcoRI E. Cleavage of isolated P22 *Eco*RI E with *Hin*dIII generates the two *Hin*dIII fragments L and M, and the two *Eco*RI/*Hin*dIII fragments d and h (data not shown). Therefore, three *Hin*dIII sites lie within P22

*Eco*RI E, and *Eco*RI/*Hin*dIII d and h in the double digest are derived from the ends of P22 *Eco*RI E.

Digestion of *Eco*RI E with *Hpa*I was used to orient *Hin*dIII L and M. P22 *Eco*RI E in this experiment was present as an insert at the *Eco*RI site in the plasmid pBR322 (Bolivar *et al.*, 1977). A *Hpa*I digest of this circular plasmid DNA contains two fragments, indicating the presence of two *Hpa*I sites in P22 *Eco*RI E since there are no *Hpa*I cleavage sites in pBR322 (Bolivar *et al.*, 1977). When the recombinant plasmid is digested with *Hin*dIII and *Eco*RI, the expected P22 *Hin*dIII fragments L and M and double digestion fragments d and h appear. Subsequent digestion of the *Eco*RI/*Hin*dIII digest with *Hpa*I removes *Hin*dIII M and *Eco*RI/*Hin*dIII d (data not shown). Thus the two *Hpa*I sites in *Eco*RI E lie in *Hin*dIII M and *Eco*RI/*Hin*dIII d.

The two *Hpa*I fragments of the recombinant plasmid were separated by preparative scale agarose gel electrophoresis, recovered from the gel as described under Materials and Methods, and digested with *Hin*dIII. P22 *Hin*dIII L is obtained from the large *Hpa*I fragment (containing the pBR322 vector sequences as well as part of the P22 insert) and not from the small *Hpa*I fragment (data not shown). Thus P22 *Hin*dIII M and P22 *Eco*RI/*Hin*dIII d must be adjacent. This result establishes the fragment order within *Eco*RI E as *Eco*RI/*Hin*dIII d, *Hin*dIII M, *Hin*dIII L, and *Eco*RI/*Hin*dIII h as illustrated in Fig. 5.

HindIII cleavage products of P22 EcoRI F and G. Since P22 *Eco*RI fragments F and G are of similar size, it was difficult to prepare one fragment free of the other by preparative scale gel electrophoresis as described under Materials and Methods. Therefore, the *Hin*dIII cleavage products of pooled *Eco*RI fragments F and G eluted from an agarose gel were analyzed. The appearance of *Hin*dIII fragments K and N, and the loss of both *Eco*RI F and G in an *Eco*RI/*Hin*dIII digestion (data not shown) indicates the presence of at least four *Hin*dIII cleavage sites within *Eco*RI fragments F and G. P22 *Eco*RI G sequences free of P22 *Eco*RI F were obtained in a plasmid derivative of pBR322 into which P22 *Eco*RI G was inserted by *in vitro* ligation of *Eco*RI termini. *Hin*dIII digests of this plasmid contain P22 *Hin*dIII K and N, and *Eco*RI/*Hin*dIII i. Therefore, three *Hin*dIII targets are contained within P22 *Eco*RI G. Two new fragments should be generated by *Hin*dIII digestion of *Eco*RI G, but only *Eco*RI/*Hin*dIII i is seen. Since the sum of the molecular weights of *Hin*dIII K and N and *Eco*RI/*Hin*dIII i is approximately equal to the size of *Eco*RI G, the second double digestion fragment (designated j) is probably too small to be resolved in the gel electrophoresis systems used. The order of the three *Hin*dIII sites in *Eco*RI G, and the single site in *Eco*RI F are described below.

Order of HindIII sites within P22 EcoRI fragments A, G, and F. *Hin*dIII digestion of isolated P22 *Eco*RI F and G did not allow precise mapping of the four *Hin*dIII sites identified as internal to these fragments. In addition, *Hin*dIII digestion of *Eco*RI A did not locate four of the six *Hin*dIII sites within *Eco*RI A. The positions of *Hin*dIII sites internal to *Eco*RI fragments F, G, and A were determined by analyzing fragments produced by *Hin*dIII cleavage of segments of these *Eco*RI fragments present as substitutions in chromosomes of the related *E. coli* bacteriophage λ. These viable hybrid bacteriophages are products of recombination between λ and P22 *in vivo*.

(a) *Hin*dIII cleavage site map of λ*imm*-P22hyl. The P22 substitution in λ*imm*P22hyl (Fig. 3) contains P22 genes 24, *c*2, 18, and 12 in place of the λ genes N, *c*I, O, and P of analogous function (Botstein and Herskowitz, 1974). The position of *Eco*RI cleavage sites in this hybrid have been determined previously (Jackson *et al.*, 1978a) and are shown in Fig. 3. Figure 2c shows that the *Hin*dIII digest of λ*imm*P22hyl DNA contains eight fragments. Four of these are equivalent to λ *Hin*dIII fragments A, D, E, and F, as expected from the previous study of this hybrid (Jackson *et al.*, 1978a). Three more of the fragments are identified by their electrophoretic mobility as P22 *Hin*dIII fragments F, G, and J. Thus these three *Hin*dIII fragments are adjacent within P22 *Eco*RI A. The *Hin*dIII fragment α, not present in a *Hin*dIII digest

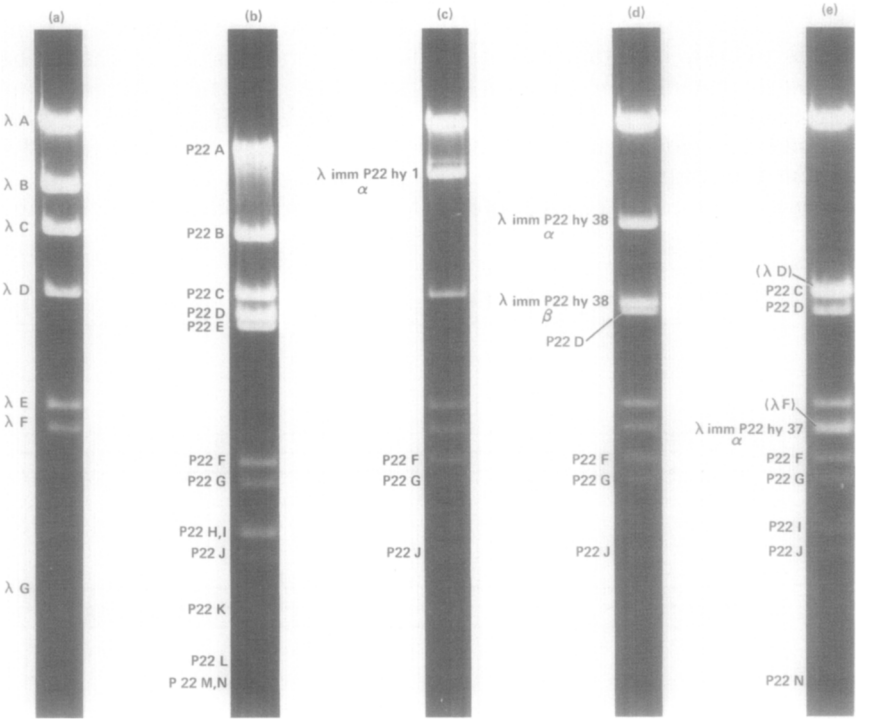

FIG. 2. Agarose gel electrophoresis of *Hin*dIII cleavage products of λ, P22, or λ*imm*P22 hybrid DNAs. (a) λDNA, (b) P22 DNA, (c) λ*imm*P22hyl DNA, (d) λ*imm*P22hy38 DNA, and (e) λ*imm*P22hy37 DNA. DNA was cleaved with *Hin*dIII and the cleavage products separated by electrophoresis in agarose gels as described under Materials and Methods. Samples were heated to 70° for 5 min just before layering on the gel in order to disrupt hydrogen bonding between λ cohesive ends. P22 and λ*imm*P22 bands are labeled according to the convention outlined by Jackson *et al.* (1978a). λ*Hin*dIII bands are labeled as in Robinson and Landy (1977). P22 and λ bands appearing in a digest of λ*imm*P22 hybrid DNA retain the same capital letter designation as in the P22 or λ parent. Bands which appear in a digest of a λ*imm*P22 hybrid DNA but not in either a P22 or λ digest are assigned Greek letters in order of increasing electrophoretic mobility. λ DNA fragments in (c), (d), and (e) have not been labeled. P22 H and I are not resolved in (b). The fragment migrating at this position in (e) was shown to be P22 *Hin*dIII I by polyacrylamide gel electrophoresis (data not shown). In (e), P22 C and λ D comigrate, and λ*imm*P22hy37 α is not resolved from λ F.

of either λ or P22 DNA, must include a junction of the P22 substitution with λ sequences. The location of *Hin*dIII α at the left end of the substitution (Fig. 3c) is the only position consistent with the position and size of the P22 substitution determined previously (Botstein and Herskowitz, 1974; Jackson *et al.*, 1978a). No second new fragment representing the right-hand side of the substitution was found. This suggests that there is a *Hin*dIII site on the P22 chromosome at a location analogous to the position of λ *Hin*dIII site 7, and that one of the *Hin*dIII fragments of λ*imm*P22hyl which comigrate with P22 *Hin*dIII F, G, or J might in fact contain a small amount of λ DNA. Conversely, the λ*imm*P22hyl *Hin*dIII fragment which migrates like λ *Hin*dIII D might contain some P22 DNA sequences. However, the conclusion that P22 F, G, and J are adjacent on the P22 genome is substantiated by analysis of a longer P22 substitution in λ*imm*P22hy38.

(b) *Hin*dIII cleavage site map of λ*imm*-P22hy38. The P22 substitution in λ*imm*-P22hy38 extends further to the right than in λ*imm*P22hyl, since it removes λ *Eco*RI site 5, and further to the left, since it includes P22 *Eco*RI sites 6 and 7 (Fig. 3; Jackson *et al.*, 1978a). Figure 2d shows that P22

*Hin*dIII F, G, and J appear in the *Hin*dIII digest of this hybrid, confirming that all three of these fragments are adjacent on the P22 chromosome. The right hand junction of P22 and λ sequences in this hybrid occurs in *Hin*dIII fragment β, since this fragment contains a λ cohesive end able to form a hydrogen-bonded dimer with λ*Hin*dIII A (data not shown). The left hand terminus of the P22 substitution lies in the new fragment α (Fig. 3d). Since P22 *Hin*dIII D is found in the digest, it must lie adjacent to P22 *Hin*dIII F, G, or J.

(c) *Hin*dIII cleavage site map of λ*imm*-

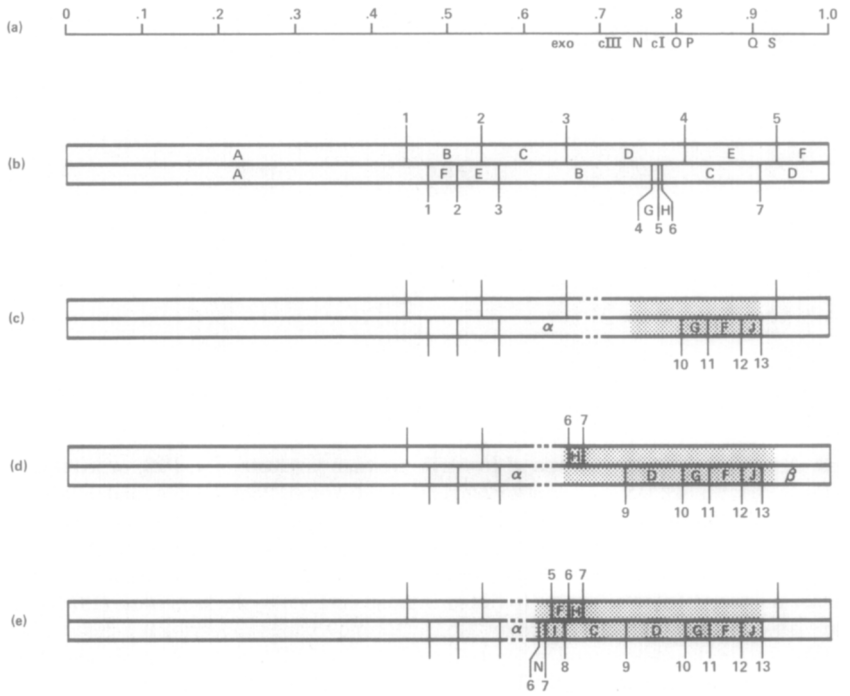

FIG. 3. *Eco*RI and *Hin*dIII cleavage site maps of λ and λ*imm*P22 hybrid phage DNAs. Maps are shown to scale. Open bars on the maps represent λ sequences, shaded bars denote P22 sequences. The dotted lines shown on the hybrid maps indicate that the P22 gene substitution was shorter than the λ DNA segment deleted. *Eco*RI cleavage sites are numbered above the map, and *Hin*dIII cleavage sites are numbered below the map. Letter designations for *Eco*RI fragments are shown in upper half of each map; *Hin*dIII fragments are labeled in lower half of maps. In (c), (d), and (e), only P22 restriction sites or fragments containing P22 DNA sequences are labeled (see Fig. 5). (a) Physical map coordinates for λ DNA. The approximate physical map positions of some λ genes replaced by P22 substitutions are shown below the scale. (b) *Eco*RI and *Hin*dIII physical gene maps of λ DNA (redrawn from Thomas and Davis, 1975; Murray and Murray, 1975; Robinson and Landy, 1977). (c) *Eco*RI and *Hin*dIII cleavage site maps of λ*imm*P22hyl DNA. The *Eco*RI physical map is redrawn from Jackson *et al.* (1978a). The P22 substitution includes P22 *Hin*dIII sites 10, 11, 12, and possibly 13 (see Fig. 5). The site labeled as P22 *Hin*dIII 13 may possibly be λ *Hin*dIII site 7 (see text). The position of the right hand end of the P22 substitution is not precisely determined but must fall in the region on the map between P22 *Hin*dIII site 12 and λ *Eco*RI site 5. (d) *Eco*RI and *Hin*dIII cleavage site map of λ*imm*P22hy38 DNA. The *Eco*RI site map is redrawn from Jackson *et al.* (1978a). The P22 substitution is shown as the minimum length consistent with the restriction fragments found. The P22 substitution includes P22 *Hin*dIII sites 9 through 13 (Fig. 5). (e) *Eco*RI and *Hin*dIII cleavage site map of λ*imm*P22hy37 DNA. The *Eco*RI site map is redrawn from Jackson *et al.* (1978a). The P22 substitution includes P22 *Hin*dIII sites 6, 7, 8, 9, 10, 11, 12, and possibly 13 (Fig. 5). The site labeled as P22 *Hin*dIII 13 may be λ *Hin*dIII site 7, since the right end of the P22 substitution may lie anywhere in the region between P22 *Hin*dIII site 12 and λ *Eco*RI site 5.

P22hy37. The P22 gene substitution in λ*imm*P22hy37 extends further to the left than that of λ*imm*P22hy38, since it includes P22 *Eco*RI site 5 (Jackson *et al.*, 1978a). It retains λ*Eco*RI site 5 at the right of the P22 substitution (Fig. 3e). Although the P22 substitution does not extend as far rightward as the substitution in λ*imm*P22hy38, the λ*imm*P22hy37 substitution still contains P22 *Hin*dIII D, thus placing *Hin*dIII D to the left of *Hin*dIII F, G, and J. In addition to P22 *Hin*dIII fragments F, G, J, and D, P22 *Hin*dIII fragments C, I, and N appear in the digest of this hybrid DNA (Fig. 2e). Thus, P22 *Hin*dIII C, I, and N lie to the left of P22 *Hin*dIII D. Neither P22 *Hin*dIII I or N can be located immediately adjacent to *Hin*dIII D, since these fragments are not produced by *Hin*dIII cleavage of purified *Eco*RI A, and *Hin*dIII I and N are shorter than *Eco*RI/*Hin*dIII c which is derived from this end of P22 *Eco*RI A. Thus, the order of *Hin*dIII fragments in this region of the P22 chromosome is (N, I), C, D, (F, G, J). P22 *Hin*dIII F, G, and J are adjacent but have not been ordered. λ*imm*-P22hy37 yields no new *Hin*dIII fragment from the right-hand end of the P22 substitution, again suggesting that P22 *Hin*dIII site 13 and λ*Hin*dIII site 7 have similar positions.

The *Hin*dIII fragments N and I are ordered by comparisons of λ*imm*P22hy37 with λ*imm*P22hy38, and consideration of the products of *Hin*dIII digestion of P22 *Eco*RI G described above. The P22 substitution in λ*imm*P22hy37 includes P22 *Eco*RI F and P22 *Hin*dIII I. *Hin*dIII I contains an *Eco*RI site (since it is not found in an *Eco*RI/*Hin*dIII digest of P22 DNA). Therefore, *Hin*dIII I contains P22 *Eco*RI site 5 (Fig. 3e). *Hin*dIII cleavage of λ*imm*P22hy37 also yields P22 *Hin*dIII N. Therefore, the order of these *Hin*dIII fragments in this region is . . . N, I, C, D . . . (Fig. 3e). Both *Hin*dIII fragments N and K are internal to P22 *Eco*RI G (see above) so the order of *Hin*dIII fragments from *Hin*dIII site 5 through site 13 is . . . K, N, I, C, D, (F, G, J) . . . .

Analysis of the three λ*imm*P22 hybrid phages has mapped four of the six *Hin*dIII cleavage sites which lie within P22 *Eco*RI A. The fragment order, counterclockwise from *Eco*RI site 7 (Fig. 5) is P22 *Eco*RI/*Hin*dIII c, *Hin*dIII D, (*Hin*dIII F, G, and J). P22 *Eco*RI/*Hin*dIII b has been identified as the other terminal fragment of *Eco*RI A. Therefore, *Hin*dIII E, also produced by *Hin*dIII cleavage of *Eco*RI A, must lie immediately adjacent to *Eco*RI/*Hin*dIII b. This position for *Hin*dIII E is substantiated by cleavage of P22 DNA with the restriction endonuclease *Sma*I (R. Deans, unpublished experiments). The *Hin*dIII cleavage products of P22 *Eco*RI A are therefore ordered as shown in Fig. 5.

HindIII Cleavage Site 3 Is Located in the ant Gene

The *ant* gene (Botstein *et al.*, 1975; Levine *et al.*, 1975) lies within one of two P22 gene clusters required for lysogeny and immunity to superinfection by P22. A portion of the *ant* gene has been shown to comprise *Hin*dIII fragment L, as described below. Weinstock and Botstein have isolated Tnl insertions in the *ant* gene of P22 (Weinstock, 1977). *Eco*RI digests of these P22 insertion mutant DNAs lack *Eco*RI fragment E, indicating that each Tnl insertion, and therefore the *ant* gene, is located within P22 *Eco*RI E (Weinstock, 1977). We have used the same insertion mutants to map the *ant* gene relative to *Hin*dIII cleavage sites.

The Tnl insertion is not cleaved by *Hin*dIII. The Tnl insertion in P22 Ap25 (gene 9) lies in *Eco*RI C (Weinstock, 1977). As shown in Fig. 4, a *Hin*dIII digest of P22 Ap25 DNA lacks *Hin*dIII B and contains a new band of molecular weight approximately 7.4 $\times 10^6$ daltons, equal to the predicted size of the Tnl insertion (3.2×10^6) in *Hin*dIII B (4.2×10^6). Therefore, the Tnl insertion in P22 Ap25 is located in *Hin*dIII B and there are no *Hin*dIII cleavage sites in Tnl.

DNA was prepared from five *ant*$^-$ phages (Ap29, Ap63, Ap4, Ap24, Ap9) carrying the Tnl mutation at different sites in the *ant* gene, and digested with *Hin*dIII and *Eco*RI plus *Hin*dIII (Fig. 4). Two of the insertion mutants (Ap24, Ap9) have altered *Hin*dIII B and *Eco*RI/*Hin*dIII h, while two more of the Tnl insertions in the *ant* gene (Ap63, Ap4) alter the mobility of

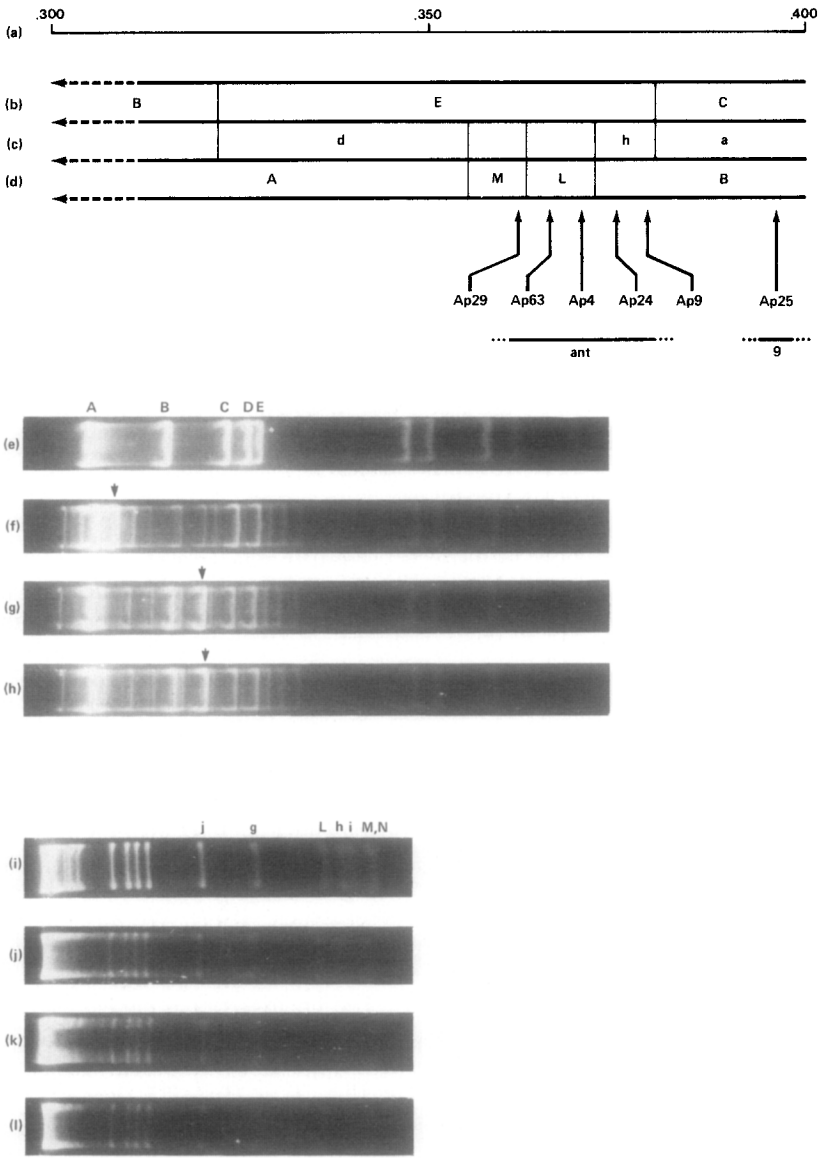

FIG. 4. Location of the *ant* gene on the *Hin*dIII cleavage site map of P22 DNA. The P22 *Hin*dIII and *Eco*RI cleavage site map between coordinates 0.3 and 0.4 (see Fig. 5) is shown to scale. (a) Physical map coordinates for P22 DNA. (b) *Eco*RI fragments of P22 DNA. (c) Fragments produced by digestion of P22 DNA with *Eco*RI plus *Hin*dIII. (d) P22 *Hin*dIII fragments. The positions of the Tnl insertions in five P22 *ant*$^-$ strains (Ap29, Ap63, Ap4, Ap24, Ap9) and one gene 9$^-$ strain (Ap25) are indicated by arrows. The Tnl insertions were located relative to *Hin*dIII sites by identifying the *Hin*dIII or *Eco*RI fragment of altered electrophoretic mobility. (e–h) Electrophoresis in 0.7% agarose gel. The direction of migration is from left to right. The arrow indicates the new *Hin*dIII fragment containing the Tnl insertion. Presence of the Tnl insertion is expected to generate additional minor bands by headful packaging of the oversized genome (Jackson *et al.*, 1978b). (e) P22 *Hin*dIII digest. (f) P22 Ap25 *Hin*dIII digest. Size of new fragment is 7.4×10^6 daltons. (g) P22 Ap29 *Hin*dIII digest. Size of new fragment is 3.4×10^6 daltons. (h) P22 Ap63 *Hin*dIII digest. Size of new fragment is 3.4×10^6 daltons. (i–l) Electrophoresis in 4% polyacrylamide gel. The direction of migration is from left to right. (i) P22 *Eco*RI plus *Hin*dIII digest. (j) P22 Ap29 *Eco*RI plus *Hin*dIII digest. P22 *Hin*dIII M is missing. (k) P22 Ap63 *Eco*RI plus *Hin*dIII digest. P22 *Hin*dIII L is missing. (l)

*Hin*dIII L. One Tnl insertion (Ap29) occurs in *Hin*dIII M. The location of these insertion mutations relative to *Hin*dIII sites is shown in Fig. 4. Since all five insertions occurred in *ant* (Weinstock, 1977), *Hin*dIII cleaves in the *ant* gene at site 2 and 3, and *ant* gene sequences are contained on *Hin*dIII M and L and *Eco*RI/*Hin*dIII h.

DISCUSSION

*Hin*dIII cleavage sites on P22 DNA have been mapped relative to the positions of *Eco*RI sites on the P22 chromosome (Jackson *et al.*, 1978a, b). The cleavage site map of the P22 genome is circular since P22 linear chromosomes are circularly permuted (Tye *et al.*, 1974a, b; Jackson *et al.*, 1978b). *Hin*dIII cleavage of P22 DNA produces 14 fragments (Fig. 1) and the map coordinates for nine of these cleavage sites (*Hin*dIII sites 4, 5, 6, 7, 8, 9, 10, 13, 14) were directly obtained from the results presented here. These experiments also show the approximate location of the remaining five *Hin*dIII cleavage sites. Three of these sites can be precisely located on the cleavage map from the following considerations. *Hin*dIII sites 1, 2, and 3 (Fig. 5) were mapped within P22 *Eco*RI E by digestion of *Eco*RI E with *Hin*dIII or *Hpa*I, but those experiments did not distinguish between the two possible orientations of *Eco*RI E. The molecular weights of products of *Hin*dIII plus *Eco*RI digestion of P22 DNA (Table 1) orient *Eco*RI as shown in Fig. 5. *Hin*dIII fragment B is composed of *Eco*RI/*Hin*dIII a plus either *Eco*RI/*Hin*dIII d or h. The sum of the molecular weights of fragments a plus h is in agreement with the size of *Hin*dIII B. That *Eco*RI/*Hin*dIII h is contained in *Hin*dIII B is confirmed by the *Hin*dIII and *Eco*RI/*Hin*dIII digestions of the insertion phages Ap24, and Ap9 (Fig. 4), since the Tnl insertion in these strains alters mobility of both *Hin*dIII B and *Eco*RI/*Hin*dIII h. Thus, *Hin*dIII sites 1, 2, and 3 are assigned the coordinates shown in Table 2 and Fig. 5.

*Hin*dIII fragment A is defined by *Hin*dIII cleavage sites 1 and 14 (Fig. 5). The *pac* site at which sequential headful packaging of P22 begins is located internal to *Hin*dIII A near site 14 (Jackson *et al.*, 1978b). The length of an average headful is greater than the length of one complete set of P22 genes (Tye *et al.*, 1974a, b) and the direction of packaging is counterclockwise relative to Fig. 5 (Jackson *et al.*, 1978b). Thus, *Hin*dIII A is never found intact in a *Hin*dIII digest of P22 wild-type DNA, and it appears heterogeneous in size in Fig. 1c. This result is additional evidence for the location of *pac* and the direction of sequential packaging determined previously (Jackson *et al.*, 1978b).

P22 *Hin*dIII fragment H is placed as shown in Fig. 5 since it is the size predicted from the coordinates for sites 4 and 5; it is removed by the P22 bp5 deletion, and it is not present in the P22 substitution in λ*imm*P22hy37.

These experiments have positioned *Hin*dIII F, J, and G between *Hin*dIII cleavage sites 10 and 13, but have not ordered these three fragments and, therefore, have not precisely located *Hin*dIII sites 11 and 12. That *Hin*dIII G is adjacent to *Hin*dIII D was shown by Berkner and Folk who studied the cleavage of 5-bromouracil-substituted P22 DNA by *Hin*dIII (K. Berkner, 1977). *Hin*dIII digests of P22 DNA containing 5-bromouracil have *Hin*dIII fragments D and G in reduced yield and contain a new fragment whose molecular weight equals the sum of the sizes of *Hin*dIII D and G. High concentrations of *Hin*dIII reduce the amount of the new fragment and concomitantly increase the yield of both *Hin*dIII D and G. These results indicate that *Hin*dIII D and G are adjacent and that 5-bromouracil substitution reduces susceptibility of site 10 to *Hin*dIII cleavage (K. Berkner, 1977).

P22 Ap9 *Eco*RI plus *Hin*dIII digest. P22 *Eco*RI/*Hin*dIII h is missing. P22 Ap4 yields the same fragments as shown in (h) and (k). P22 Ap9 yields the same *Hin*dIII fragments as (f). P22 Ap24 yields the same *Hin*dIII fragments as (f), and the same *Eco*RI/*Hin*dIII fragments as (l). Since P22 *Hin*dIII M and N comigrate during electrophoresis in a 4% polyacrylamide gel (see Fig. 1), retention of *Hin*dIII N in the Ap29 insertion mutant obscures loss of *Hin*dIII M [see (j) above], although the new fragment created by the Tnl insertion in *Hin*dIII M is seen in (g) above.

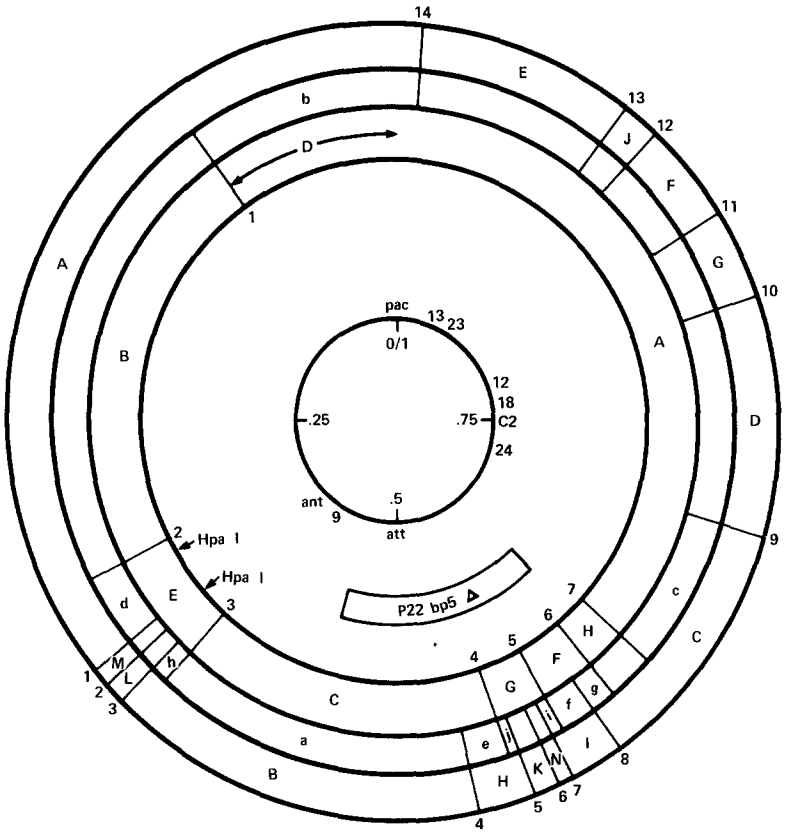

FIG. 5. *Hin*dIII and *Eco*RI cleavage site maps of P22 DNA. *Hin*dIII and *Eco*RI fragment maps are shown to scale as three concentric rings. *Hin*dIII cleavage sites are numbered outside the outer ring (*Hin*dIII fragment map) and *Eco*RI sites are numbered inside the inner ring (*Eco*RI fragment map redrawn from Jackson *et al.*, (1978a) with physical map coordinates re-aligned to originate at *pac*. The middle of the three rings shows the order of fragments produced by *Eco*RI plus *Hin*dIII cleavage. *Eco*RI fragment D is a segment of *Eco*RI A generated by P22 DNA maturation (Jackson *et al.*, 1978b). The two *Hpa*I sites in *Eco*RI E at coordinates .331 and .360 are shown. Other *Hpa*I sites in P22 DNA have not been mapped. The position of the bp5 deletion is indicated by the bar extending from .46 to .62. The small inner circle indicates physical location of some P22 genes determined in this work (see Discussion). Positions of *att* and *pac* are from Jackson *et al.* (1978a, b); gene 9 location from Weinstock (1977).

*Hin*dIII site 11 is therefore located at coordinate .832. Although these data do not distinguish between the two possible orders of *Hin*dIII F and J cleavage with *Hpa*I and *Pst*I locate *Hin*dIII site 12 at coordinate .876 (R. Deans, unpublished data). The 14 *Hin*dIII cleavage sites have now been mapped relative to *Eco*RI sites on P22 DNA as shown in Fig. 5. The coordinates of the cleavage sites are listed in Table 2.

Since some P22 genes have been located on the P22 *Eco*RI cleavage site map (Jackson *et al.*, 1978a), the *Hin*dIII cleavage map can also be aligned with the genetic map (Fig. 5). In addition, our results assign some P22 genes to individual *Hin*dIII fragments. Six of the *Hin*dIII sites subdivide the P22 *Eco*RI fragment A which comprises almost half the P22 genome and contains most P22 early genes as well as some late genes (Jackson *et al.*, 1978a). P22 early genes *c*2, 24, 18, and 12 lie between P22 *Hin*dIII sites 9 and 13 since these P22 genes are present in λ*imm*P22hyl. Heteroduplex analysis of λ*imm*P22hyl (Botstein and Herskowitz, 1974) together with the *Hin*dIII map of λ*imm*P22hyl (Fig. 3b) assign *c*2, 24, 18, and 12 to *Hin*dIII D, pos-

sibly extending into *Hin*dIII G. *Hin*dIII cleavage site mapping of the hybrid phage DNAs also places P22 gene 13 on *Hin*dIII E (see Fig. 3d) and suggests that *Hin*dIII site 13 might be located within P22 gene 23, a regulatory gene which is analogous in map location to λ gene Q (Botstein *et al.*, 1972).

P22 has two immunity regions, one at a position in the map analogous to the position of the single λ immunity region, and another (*imm*I), for which no λ analog exists, located between phage head and tail genes (Levine *et al.*, 1975; Botstein *et al.*, 1975). *Hin*dIII sites 1, 2, and 3, as well as two *Hpa*I sites (Fig. 5) subdivide the *imm*I region into fragments about the size of a single gene or smaller. Gene *ant* in the *imm*I region codes for an antirepressor protein which antagonizes the function of the P22 phage repressor (Susskind and Botstein, 1975). Insertion mutations which inactivate *ant* gene function (Weinstock, 1977) have been mapped to *Hin*dIII fragments M, L, and *Eco*RI/*Hin*dIII fragment h. Since the P22 Ap29 insertion is in *Hin*dIII M and the P22 Ap9 insertion is in *Eco*RI/*Hin*dIII h, *Hin*dIII L must consist entirely of *ant* gene sequences, and there are two *Hin*dIII cleavage sites within the *ant* gene. The size of the *ant* gene polypeptide is 27,000 daltons (Susskind and Botstein, 1978), and therefore, the minimum size of the *ant* gene is about 0.45×10^6 daltons. These three fragments therefore should contain most if not all of the *ant* gene.

The map of *Hin*dIII and *Eco*RI cleavage sites reported here is a detailed physical map of the P22 genome. This cleavage site map is aligned with the P22 genetic map, and some P22 genes have been precisely located on the physical map. The abundance of cleavage sites in the early gene region and in the *imm*I region will be valuable tools in studies of P22 regulatory mechanisms.

TABLE 2

MAP COORDINATES OF *Eco*RI AND *Hin*dIII CLEAVAGE SITES ON P22 DNA[a]

P22 *Eco*RI site	Map position	P22 *Hin*dIII site	Map position
1	.096	1	.353
2	.318	2	.36
3	.376	3	.368
4	.550	4	.530
5	.576	5	.554
6	.603	6	.566
7	.623	7	.573
		8	.596
pac	0	9	.699
		10	.795
		11	.832
		12	.876
		13	.894
		14	.982

[a] P22 *Eco*RI map coordinates are calculated from the molecular weights reported by Jackson *et al.* (1978a,b), and a total genome size of 27.45×10^6 daltons. The P22 *Hin*dIII map coordinates were calculated from the data of Table 1, the fragment order of Fig. 5 and a total genome size of 27.23×10^6 daltons, but the origin of the coordinate system has been changed from *Eco*RI site 1 to *pac*. Cleavage site coordinates are calculated to three significant figures to indicate the order of sites located close together.

ACKNOWLEDGMENTS

We are grateful to William Folk and David Mason for their kind gifts of restriction endonucleases and Rex Chisholm, David Jackson, and Robert Deleys for discussion during the course of this work. We thank David Botstein, George Weinstock, Kathleen Berkner, and William Folk for their communication of unpublished results. This study was supported by Grant AI-12369 from the National Institutes of Health. RJD was supported in part by Institutional Research Grant IN-40Q to the University of Michigan from the American Cancer Society.

REFERENCES

BERKNER, K. (1977). "Quantitative Analysis of Restriction Enzymes: Methylase Specificities, and Application of the Polynucleotide Kinase Exchange Reaction to Studying Endonuclease Specificities." Ph.D. thesis, The University of Michigan, Ann Arbor.

BOLIVAR, F., RODRIGUEZ, R. L., GREEN, P. J., BETLACH, M. C., HEYNEKER, H. L., BOYER, H. W., CROSA, J. H., and FALKOW, S. (1977). The circular restriction map of pBR322. *In* "DNA Insertion Elements, Plasmids, and Episomes" (A. I. Bukhari, J. A. Shapiro, and S. L. Adhya, eds.), pp. 686–687. Cold Spring Harbor Press, Cold Spring Harbor, N. Y.

BOTSTEIN, D., CHAN, R. K., and WADDELL, C. H. (1972). The genetics of bacteriophage P22. II. Gene order and gene function. *Virology* **49**, 268–282.

BOTSTEIN, D., and HERSKOWITZ, I. (1974). Properties

of hybrids between *Salmonella* phage P22 and coliphage Lambda. *Nature (London)* **251**, 584–589.

BOTSTEIN, D., LEW, K. K., JARVIK, V., and SWANSON, C. A., JR. (1975) Role of antirepressor in the bipartite control of repression and immunity by bacteriophage P22. *J. Mol. Biol.* **91**, 439–462.

CHAN, R. K., and BOTSTEIN, D. (1976). Specialized transduction by bacteriophage P22 in *Salmonella typhimurium*: Genetic and physical structure of the transducing genomes and the prophage attachment site. *Genetics* **83**, 443–458.

COLLINS, C. J., JACKSON, D. A., and DEVRIES, F. A. J. (1976). Biochemical construction of specific chimeric plasmids from ColEl DNA and unfractionated *Escherichia coli* DNA. *Proc. Nat. Acad. Sci. USA* **73**, 3838–3842.

DELEYS, R. J., and JACKSON, D. A. (1976). Electrophoretic analysis of covalently closed SV40 DNA: Boltzman distribution of DNA species. *Nucl. Acids Res.* **3**, 641–652.

HEFFRON, F., RUBENS, C., and FALKOW, S. (1975). Translocation of a plasmic DNA sequence which mediates ampicillin resistance: Molecular nature and specificity of insertion. *Proc. Nat. Acad. Sci. USA* **72**, 3623–3628.

HERNALSTEENS, J., VILLARROEL-MANDIOLA, R., VAN MONTAGU, M., and SCHELL, J. (1977). Transposition of Tnl to a broad-host-range drug resistance plasmid. *In* "DNA Insertion Elements, Plasmids, and Episomes" (A. I. Bukhari, J. A. Shapiro, and S. L. Adhya, eds.), pp. 179–183. Cold Spring Harbor Press, Cold Spring Harbor, N. Y.

HILLIKER, S. (1974). "Specificity of Regulatory Elements in Temperate Bacteriophages." Ph.D. thesis. Massachusetts Institute of Technology, Cambridge.

JACKSON, E. N., MILLER, H. I., and ADAMS, M. A (1978a). *Eco*RI restriction endonuclease cleavage site map of bacteriophage P22 DNA. *J. Mol. Biol.* **118**, 347–363.

JACKSON, E. N., JACKSON, D. A., and DEANS, R. J. (1978b). *Eco*RI analysis of bacteriophage P22 DNA packaging. *J. Mol. Biol.* **118**, 365–388.

LAI, C. J., and NATHANS, D. (1974). Deletion mutants of SV40 generated by enzymatic excision of DNA segments from the viral genome. *J. Mol. Biol.* **89**, 179–193.

LEVINE, M., TRUESDELL, S., RAMAKRISHNAN, T., and BRONSON, M. J. (1975). Dual control of lysogeny of bacteriophage P22: An antirepressor locus and its controlling elements. *J. Mol. Biol.* **91**, 421–438.

MURRAY, K., and MURRAY, N. (1975). Phage lambda receptor chromosomes for DNA fragments made with restriction endonuclease III of *Haemophilus influenzae* and restriction endonuclease I of *E. coli*. *J. Mol. Biol.* **98**, 551–564.

NATHANS, D., and SMITH, H. O. (1975). Restriction endonucleases in the analysis and restructuring of DNA molecules. *Annu. Rev. Biochem.* **44**, 273–293.

ROBINSON, L. H., and LANDY, A. (1977) *Hin*dII, *Hin*dIII, and *Hpa*I restriction fragment maps of bacteriophage lambda DNA. *Gene* **2**, 1–31.

SMITH, H. O., and NATHANS, D. (1973). A suggested nomenclature for bacterial host modification and restriction systems and their enzymes. *J. Mol. Biol.* **81**, 419–423.

SUSSKIND, M., and BOTSTEIN, D. (1975). Mechanism of action of *Salmonella* phage P22 antirepressor. *J. Mol. Biol.* **98**, 413–424.

SUSSKIND, M., and BOTSTEIN, D. (1978). Molecular genetics of bacteriophage P22. *Microbiol. Rev.* **42**, 385–413.

THOMAS, M., and DAVIS, R. W. (1975). Studies on the cleavage of bacteriophage lambda DNA with *Eco*RI restriction endonuclease. *J. Mol. Biol.* **91**, 315–328.

TYE, B.-K., CHAN, R. K., and BOTSTEIN, D. (1974a). Packaging of an oversize transducing genome by *Salmonella* phage P22. *J. Mol. Biol.* **85**, 485–500.

TYE, B.-K., HUBERMAN, J. A., and BOTSTEIN, D. (1974b). Non-random circular permutation of phage P22 DNA. *J. Mol. Biol.* **85**, 501–532.

WEINSTOCK, G. M. (1977). "Genetic and Physical Studies of Bacteriophage P22 Genomes Containing Translocatable Drug Resistance Elements." Ph.D. thesis, Massachusetts Institute of Technology, Cambridge.

ZISSLER, J., SIGNER, E., and SCHAEFER, F. (1971). The role of recombination in growth of bacteriophage lambda II. Inhibition of growth by prophage P2. *In* "The Bacteriophage Lambda" (A. D. Hershey ed.), pp. 469–476. Cold Spring Harbor Press, Cold Spring Harbor, N. Y.